SCIENCE CHINA
Information Sciences

• RESEARCH PAPER •
Special Focus on Advanced Nonlinear Control of Hypersonic Flight Vehicles

July 2015, Vol. 58 070203:1–070203:9
doi: 10.1007/s11432-015-5328-4

Composite dynamic surface control of hypersonic flight dynamics using neural networks

ZHANG ShangMin[1]*, LI ChunWen[1] & ZHU JiHong[2]

[1]*Department of Automation, Tsinghua University, Beijing* 100084*, China;*
[2]*Department of Computer Science and Technology, Tsinghua University, Beijing* 100084*, China*

Received January 24, 2015; accepted March 1, 2015; published online May 20, 2015

Abstract This paper addresses the composite neural tracking control for the longitudinal dynamics of hypersonic flight dynamics. The dynamics is decoupled into velocity subsystem, altitude subsystem, and attitude subsystem. For the altitude subsystem, the reference command of flight path angle is derived for the attitude subsystem. To deal with the system uncertainty and provide efficient neural learning, the composite law for neural weights updating is studied with both tracking error and modeling error. The uniformly ultimate boundedness stability is guaranteed via Lyapunov approach. Under the dynamic surface control with novel neural design, the neural system converges in a faster mode and better tracking performance is obtained. Simulation results are presented to show the effectiveness of the design.

Keywords hypersonic flight vehicle, composite dynamic surface control, neural network, longitudinal dynamics, stability

Citation Zhang S M, Li C W, Zhu J H. Composite dynamic surface control of hypersonic flight dynamics using neural networks. Sci China Inf Sci, 2015, 58: 070203(9), doi: 10.1007/s11432-015-5328-4

1 Introduction

With high-speed flying, hypersonic flight vehicles (HFVs) provide a promising and cost-effective technology to fulfill the need of commercial as well as military applications for space access and prompt global reach capabilities. As discussed in [1], due to the highly coupled and nonlinear nature of the dynamic behavior, the design of flight control systems for such kind of flight vehicles poses many challenges.

Currently, the focus is lying on control [2–4] of the longitudinal models such as winged-cone model [5] and control oriented model (COM) [6]. In [7,8], the linear design is analyzed by linearizing the nonlinear dynamics at the trim state. In [9], the sliding mode control (SMC) is designed for hypersonic flight dynamics at 110,000 ft and Mach 15. With the same model, in [10,11], the disturbance-observer-based controller is analyzed. In [12], the adaptive controller design with high gain observer is constructed where the lumped system uncertainty is approximated by neural networks (NNs). In [13], using intermediate models such as T–S modeling, the original dynamics is described by a set of linear equations and the adaptive control is constructed. More details of recent progress in hypersonic flight control could be found in [1].

* Corresponding author (email: zhang-sm09@mails.tsinghua.edu.cn)

It is noted that for highly nonlinear dynamics, with small perturbation design or input/output linearization, the derived dynamics might be quite different from the characteristics of original system. Recently, more and more emphasis is on nonlinear control by decoupling the dynamics into several subsystems so that the controller could be designed specifically for each subsystem and the problem of dealing with uncertainty or disturbance could be done step by step. Once for each step the design is completed, in the last step the uncertainty will not be cumulated.

Back-stepping is an efficient method for systematic design and it has been applied on flight control [14, 15]. The back-stepping design with parameter learning of the linearly parameterized dynamics is studied in [16]. To deal with the "explosion of the complexity" of the back-stepping design, dynamic surface control (DSC) design is analyzed in [17,18] by letting the signal pass though the filter. However, in reality it is difficult to obtain the linearly parameterized dynamics since there is less flight data. In [19], the adaptive discrete back-stepping is applied on the dynamics using the nominal information of the nonlinearities and in [20], the flexible dynamics with input nonlinearity is studied. In case of unknown dynamics, intelligent control [21,22] could be employed. In [23], the fuzzy DSC design is applied on the winged-cone model.

Recently, the composite neural design [24] using both tracking error and NN modeling error is proposed where faster adaptation and better tracking performance are achieved. Inspired by the idea in [24], we analyze the composite neural control of longitudinal dynamics for HFV. The dynamics is transformed into the strict-feedback form and then the command filter-based DSC design is presented with composite learning algorithm.

This paper is organized as follows. Section 2 describes the longitudinal dynamics and the functional decomposition. Sections 3 and 4 present the adaptive controller design and the stability analysis. The simulation results are included in Section 5. Section 6 presents several comments and final remarks.

2 Model dynamics and problem formulation

2.1 Hypersonic flight dynamics

The COM of a generic HFV considered in this study is given by [6]. The equations are listed as follows:

$$\dot{V} = \frac{T\cos\alpha - D}{m} - g\sin\gamma, \tag{1}$$

$$\dot{h} = V\sin\gamma, \tag{2}$$

$$\dot{\gamma} = \frac{L + T\sin\alpha}{mV} - \frac{g\cos\gamma}{V}, \tag{3}$$

$$\dot{\alpha} = q - \dot{\gamma}, \tag{4}$$

$$\dot{q} = \frac{M_{yy}}{I_{yy}}. \tag{5}$$

The dynamics is presented with five state variables $X_h = [V, h, \alpha, \gamma, q]^{\mathrm{T}}$ and two control inputs $U = [\delta_e, \Phi]^{\mathrm{T}}$, where V is the velocity, γ is the flight path angle (FPA), h is the altitude, α is the attack angle, q is the pitch rate, δ_e is elevator deflection, and Φ is the fuel equivalence ratio.

In (1)–(5), T, D, L, and M_{yy} represent thrust, drag, lift-force, and pitching moment, respectively, and have the following expressions:

$$\begin{aligned}
&T = T_\Phi(\alpha)\Phi + T_0(\alpha) \approx [\beta_1\Phi + \beta_2]\,\alpha^3 + [\beta_3\Phi + \beta_4]\,\alpha^2 + [\beta_5\Phi + \beta_6]\,\alpha + [\beta_7\Phi + \beta_8]\,,\\
&D \approx \bar{q}S(C_D^{\alpha^2}\alpha^2 + C_D^{\alpha}\alpha + C_D^0),\\
&L = L_0 + L_\alpha\alpha \approx \bar{q}SC_L^0 + \bar{q}SC_L^\alpha\alpha,\\
&M_{yy} = M_T + M_0(\alpha) + M_{\delta_e}\delta_e \approx z_T T + \bar{q}S\bar{c}(C_M^{\alpha^2}\alpha^2 + C_M^\alpha\alpha + C_M^0) + \bar{q}S\bar{c}C_M^{\delta_e}\delta_e,\\
&\bar{q} = \frac{1}{2}\rho V^2, \rho = \rho_0\exp\left[-\frac{h-h_0}{h_s}\right].
\end{aligned}$$

More related information of this model can be found in [6,17].

2.2 Dynamics transformation

For the velocity subsystem (1), we have

$$\dot{V} = g_v \Phi + f_v - g \sin \gamma \tag{6}$$

with $f_v = \frac{T_0 \cos \alpha - D}{m}$, $g_v = \frac{T_\Phi \cos \alpha}{m}$.

Assumption 1 ([19])**.** The thrust term $T \sin \alpha$ in (3) can be neglected because it is generally much smaller than L.

Lemma 1 ([12])**.** For the altitude subsystem, the altitude tracking error is defined as $\tilde{h} = h - h_r$ and the FPA command is chosen as

$$\gamma_d = \frac{-k_h (h - h_r) - k_i \int (h - h_r) \, \mathrm{d}t + \dot{h}_r}{V}. \tag{7}$$

If $k_h > 0$ and $k_i > 0$ are chosen and the FPA is controlled to follow γ_d, the altitude tracking error is regulated to zero exponentially.

Define $X = [x_1, x_2, x_3]^{\mathrm{T}}$, $x_1 = \gamma$, $x_2 = \theta_p$, $x_3 = q$, where $\theta_p = \alpha + \gamma$. The attitude subsystem [12] can be derived as

$$\begin{cases} \dot{x}_1 = f_1 (x_1) + g_1 x_2, \\ \dot{x}_2 = x_3, \\ \dot{x}_3 = f_3 (X) + g_3 u, \\ u = \delta_e, \end{cases} \tag{8}$$

where $f_1 = \frac{L_0 - L_\alpha \gamma}{mV} - \frac{g}{V} \cos x_1$, $g_1 = \frac{L_\alpha}{mV}$, $f_3 = \frac{M_T + M_0(\alpha)}{I_{yy}}$, $g_3 = \frac{M_{\delta_e}}{I_{yy}}$.

Assumption 2. For $i = 1, 3$, the nonlinearities f_i are unknown and the control gain functions g_i are considered as known.

3 Composite attitude dynamic surface control with prediction error

The controller design for attitude subsystem is on DSC scheme where virtual control will be designed step by step. Different from previous design in [17], the neural design is presented. Furthermore, the composite learning will be constructed using NN modeling error with the design in [24].

Step 1: Considering the first equation of FPA in (8), we know

$$\dot{x}_1 = f_1(x_1) + g_1 x_2 = \omega_1^{*\mathrm{T}} \theta_1(x_1) + \varepsilon_1 + g_1 x_2, \tag{9}$$

where ω_1^* is the optimal NN weights vector to approximate f_1 and ε_1 is the NN approximation error satisfying $| \varepsilon_1 | \leqslant \varepsilon_M$.

Define the FPA tracking error

$$e_1 = x_1 - x_1^d, \tag{10}$$

where $x_1^d = \gamma_d$.

Design virtual control x_2^d as

$$x_2^d = \frac{-\hat{\omega}_1^{\mathrm{T}} \theta_1(x_1) - k_1 e_1 + \dot{x}_1^d}{g_1}, \tag{11}$$

where $\hat{\omega}_1$ is the estimation of ω_1^* and $k_1 > 0$ is the design constant.

Introduce a new state variable x_2^c and let x_2^d pass through a first-order filter with time constant $\alpha_2 > 0$ to obtain x_2^c

$$\alpha_2 \dot{x}_2^c + x_2^c = x_2^d, \ x_2^c(0) = x_2^d(0). \tag{12}$$

Define $e_2 = x_2 - x_2^c$. Then, the derivative of e_1 is obtained as

$$\dot{e}_1 = \dot{x}_1 - \dot{x}_1^d = \omega_1^{*\mathrm{T}} \theta_1(x_1) + \varepsilon_1 + g_1 x_2 - \dot{x}_1^d = \tilde{\omega}_1^{\mathrm{T}} \theta_1(x_1) + \varepsilon_1 - k_1 e_1 + g_1 e_2 + g_1 (x_2^c - x_2^d), \tag{13}$$

where $\tilde{\omega}_1 = \omega_1^* - \hat{\omega}_1$.

To remove the effect of the known error $(x_2^c - x_2^d)$, the compensating signal z_1 is designed as

$$\dot{z}_1 = -k_1 z_1 + g_1 z_2 + g_1(x_2^c - x_2^d),\ z_1(0) = 0, \tag{14}$$

where z_2 will be defined in the next step.

Now we obtain the compensated tracking error signals

$$\nu_1 = e_1 - z_1,\ \nu_2 = e_2 - z_2. \tag{15}$$

Define the prediction error as

$$z_{1\mathrm{NN}} = x_1 - \hat{x}_1, \tag{16}$$

where the signal $\hat{x}_1$ is defined with the serial–parallel estimation model [25,26]:

$$\dot{\hat{x}}_1 = \hat{\omega}_1^{\mathrm{T}}\theta_1(x_1) + g_1 x_2 + \beta_1 z_{1\mathrm{NN}},\ \hat{x}_1(0) = x_1(0) \tag{17}$$

with $\beta_1 > 0$ as the user-defined positive constant.

For the NN updating law, the signal $z_{1\mathrm{NN}}$ is employed to construct the learning design

$$\dot{\hat{\omega}}_1 = \gamma_1\left[(\nu_1 + \gamma_{z1} z_{1\mathrm{NN}})\,\theta_1(x_1) - \delta_1\hat{\omega}_1\right], \tag{18}$$

where γ_1, γ_{z1}, and δ_1 are positive design constants.

Step 2: Considering the second equation of pitch angle in (8), we know

$$\dot{x}_2 = x_3. \tag{19}$$

The virtual control x_3^d is designed as

$$x_3^d = -k_2 e_2 - g_1 e_1 + \dot{x}_2^c, \tag{20}$$

where $k_2 > 0$ is the design constant.

Introduce a new state variable x_3^c and let x_3^d pass through a first-order filter with time constant $\alpha_3 > 0$ to obtain x_3^c

$$\alpha_3\dot{x}_3^c + x_3^c = x_3^d,\ x_3^d(0) = x_3^c(0). \tag{21}$$

Then, the derivative of e_2 is calculated as

$$\dot{e}_2 = \dot{x}_2 - \dot{x}_2^c = -k_2 e_2 - g_1 e_1 + e_3 + (x_3^c - x_3^d). \tag{22}$$

To remove the effect of the known error $(x_3^c - x_3^d)$, the compensating signal z_2 is defined as

$$\dot{z}_2 = -k_2 z_2 - g_1 z_1 + z_3 + (x_3^c - x_3^d),\ z_2(0) = 0, \tag{23}$$

where z_3 will be defined in the next step.

Define the compensated tracking error signal

$$\nu_2 = e_2 - z_2. \tag{24}$$

Step 3: Considering the third equation in (8) and using NN to approximate $f_3(X)$, we know

$$\dot{x}_3 = f_3(X) + g_3 u = \omega_3^{*\mathrm{T}}\theta_3(X) + \varepsilon_3 + g_3 u, \tag{25}$$

where ω_3^* is the optimal NN weights vector and ε_3 is the NN approximation error with $|\,\varepsilon_3\,| \leqslant \varepsilon_M$.

Define the third error surface e_3 to be

$$e_3 = x_3 - x_3^c. \tag{26}$$

The elevator deflection u is designed as

$$u = \frac{-\hat{\omega}_3^{\mathrm{T}}\theta_3(X) - k_3 e_3 - e_2 + \dot{x}_3^c}{g_3}, \tag{27}$$

where $\hat{\omega}_3$ is the estimation of ω_3^* and $k_3 > 0$ is the design constant.

Then, the derivative of e_3 is obtained as

$$\dot{e}_3 = \dot{x}_3 - \dot{x}_3^c = \tilde{\omega}_3^{\mathrm{T}}\theta_3(X) + \varepsilon_3 - k_3 e_3 - e_2, \tag{28}$$

where $\tilde{\omega}_3 = \omega_3^* - \hat{\omega}_3$.

The compensating signal is defined as

$$\dot{z}_3 = -k_3 z_3 - z_2,\ z_3(0) = 0. \tag{29}$$

Define the compensated tracking error signal

$$\nu_3 = e_3 - z_3 \tag{30}$$

and the prediction error

$$z_{3\mathrm{NN}} = x_3 - \hat{x}_3, \tag{31}$$

where the derivative of NN modeling information is defined with the serial–parallel estimation model:

$$\dot{\hat{x}}_3 = \hat{\omega}_3^{\mathrm{T}}\theta_3(X) + g_3 u + \beta_3 z_{3\mathrm{NN}},\ \hat{x}_3(0) = x_3(0) \tag{32}$$

with $\beta_3 > 0$ as the user-defined positive constant.

The update law of $\hat{\omega}_3$ is designed to be

$$\dot{\hat{\omega}}_3 = \gamma_3\left[(\nu_3 + \gamma_{z3} z_{3\mathrm{NN}})\,\theta_3(X) - \delta_3\hat{\omega}_3\right], \tag{33}$$

where γ_3, γ_{z3}, and δ_3 are positive design constants.

Remark 1. In (14) and (23), the control gain functions $g_i, i = 1, 2$ are included to construct the compensating signals z_i.

4 Stability analysis

Theorem 1. Consider system (8) with the DSC laws defined in (11), (20), and (27), the NN adaptation laws (18), (33), and compensated error signals defined in (15), (30). The signals ν_i, $i = 1, 2, 3$, and $z_{j\mathrm{NN}}$, $\tilde{\omega}_j$, $j = 1, 3$ are guaranteed to be uniformly ultimately bounded.

Proof. The Lyapunov function is selected as

$$V = \frac{1}{2}\sum_{i=1}^{3}\nu_i^2 + \frac{1}{2}\sum_{j=1,3}\left(\gamma_{zj} z_{j\mathrm{NN}}^2 + \tilde{\omega}_j^{\mathrm{T}}\gamma_j^{-1}\tilde{\omega}_j\right). \tag{34}$$

For error dynamics of ν_i, $i = 1, 2, 3$, we have

$$\dot{\nu}_1 = \dot{e}_1 - \dot{z}_1 = \tilde{\omega}_1^{\mathrm{T}}\theta_1(x_1) + \varepsilon_1 - k_1(e_1 - z_1) + g_1(e_2 - z_2) = \tilde{\omega}_1^{\mathrm{T}}\theta_1(x_1) + \varepsilon_1 - k_1\nu_1 + g_1\nu_2, \tag{35}$$

$$\dot{\nu}_2 = \dot{e}_2 - \dot{z}_2 = -k_2(e_2 - z_2) - g_1(e_1 - z_1) + (e_3 - z_3) = -k_2\nu_2 - g_1\nu_1 + \nu_3, \tag{36}$$

$$\dot{\nu}_3 = \dot{e}_3 - \dot{z}_3 = \tilde{\omega}_3^{\mathrm{T}}\theta_3(X) + \varepsilon_3 - k_3(e_3 - z_3) - (e_2 - z_2) = \tilde{\omega}_3^{\mathrm{T}}\theta_3(X) + \varepsilon_3 - k_3\nu_3 - \nu_2. \tag{37}$$

Define $\bar{x}_j = [x_1, x_2, \ldots, x_j]^{\mathrm{T}}$. With (11), (17), (27), and (32), for $j = 1, 3$ it is known that

$$\dot{z}_{j\mathrm{NN}} = \dot{x}_j - \dot{\hat{x}}_j = \tilde{\omega}_j^{\mathrm{T}}\theta_j(\bar{x}_j) + \varepsilon_j - \beta_j z_{j\mathrm{NN}}. \tag{38}$$

Defining $m_j = \tilde{\omega}_j^{\mathrm{T}}\theta_j(\bar{x}_j)$, the following equation can be obtained as

$$\dot{z}_{j\mathrm{NN}} z_{j\mathrm{NN}} = z_{j\mathrm{NN}}\left(m_j + \varepsilon_j\right) - \beta_j z_{j\mathrm{NN}}^2. \tag{39}$$

The derivative of V is derived as

$$\begin{aligned}\dot{V} &= \sum_{j=1,3}\left(\gamma_{zj} z_{j\mathrm{NN}}\dot{z}_{j\mathrm{NN}} - \tilde{\omega}_j^{\mathrm{T}}\gamma_j^{-1}\dot{\hat{\omega}}_j\right) + \sum_{i=1}^{3}\nu_i\dot{\nu}_i \\ &= \sum_{i=1}^{3} -k_i\nu_i^2 + \sum_{j=1,3}\left[\nu_j m_j + \nu_j\varepsilon_j\right] - \sum_{j=1,3} m_j\left[\left(\nu_j + \gamma_{zj} z_{j\mathrm{NN}}\right) + \delta_j\tilde{\omega}_j^{\mathrm{T}}\hat{\omega}_j\right] \\ &\quad + \sum_{j=1,3}\left[\gamma_{zj} z_{j\mathrm{NN}}\left(m_j + \varepsilon_j\right) - \gamma_{zj}\beta_j z_{j\mathrm{NN}}^2\right] \\ &= \sum_{i=1}^{3} -k_i\nu_i^2 + \sum_{j=1,3}\left(\nu_j\varepsilon_j + \gamma_{zj} z_{j\mathrm{NN}}\varepsilon_j - \gamma_{zj}\beta_j z_{j\mathrm{NN}}^2 - \delta_j\tilde{\omega}_j^{\mathrm{T}}\tilde{\omega}_j + \delta_j\tilde{\omega}_j^{\mathrm{T}}\omega_j^*\right).\end{aligned} \tag{40}$$

Using the following facts

$$\begin{aligned}&\nu_j\varepsilon_j - k_j\nu_j^2 = -k_j\left(\nu_j - \frac{\varepsilon_j}{2k_j}\right)^2 + \frac{1}{4k_j}\varepsilon_j^2, \\ &z_{j\mathrm{NN}}\varepsilon_j - \beta_j z_{j\mathrm{NN}}^2 = -\beta_j\left(z_{j\mathrm{NN}} - \frac{\varepsilon_j}{2\beta_j}\right)^2 + \frac{1}{4\beta_j}{\varepsilon_j}^2, \\ &\tilde{\omega}_j^{\mathrm{T}}\omega_j^* - \tilde{\omega}_j^{\mathrm{T}}\tilde{\omega}_j = -\left\|\tilde{\omega}_j - \frac{\omega_j^*}{2}\right\|^2 + \frac{1}{4}\left\|\omega_j^*\right\|^2.\end{aligned}$$

Then, the derivative of V is calculated as

$$\begin{aligned}\dot{V} &= -k_2\nu_2^2 - \sum_{j=1,3}\left[k_j\left(\nu_j - \frac{\varepsilon_j}{2k_j}\right)^2 - \frac{1}{4k_j}\varepsilon_j^2\right] - \sum_{j=1,3}\gamma_{zj}\left[\beta_j\left(z_{j\mathrm{NN}} - \frac{\varepsilon_j}{2\beta_j}\right)^2 - \frac{1}{4\beta_j}\varepsilon_j^2\right] \\ &\quad - \sum_{j=1,3}\delta_j\left[\left\|\tilde{\omega}_j - \frac{\omega_j^*}{2}\right\|^2 - \frac{1}{4}\left\|\omega_j^*\right\|^2\right] \\ &\leqslant -k_2\nu_2^2 - \sum_{j=1,3}\left[k_0\left(\nu_j - \frac{\varepsilon_j}{2k_j}\right)^2 + \gamma_{z\min}\beta_0\left(z_{j\mathrm{NN}} - \frac{\varepsilon_j}{2\beta_j}\right)^2 + \delta_0\left\|\tilde{\omega}_j - \frac{\omega_j^*}{2}\right\|^2\right] + P,\end{aligned} \tag{41}$$

where for $j = 1, 3$, $k_0 = \min[k_j]$, $\beta_0 = \min[\beta_j]$, $\gamma_{z\min} = \min[\gamma_{zi}]$, $\delta_0 = \min[\delta_j]$, $P = \frac{2}{4k_0}\varepsilon_M^2 + \frac{2\gamma_{z\max}}{4\beta_0}\varepsilon_M^2 + \frac{2\delta_{\max}}{4}\omega_{\max}^2$, $\gamma_{z\max} = \max[\gamma_{zi}]$, $\omega_{\max} = \max[\|\omega_j^*\|]$, and $\delta_{\max} = \max[\delta_j]$.

For $j = 1, 3$, if $|\nu_j - \frac{\varepsilon_j}{2k_j}| \geqslant \sqrt{\frac{P}{k_0}}$ or $|z_{i\mathrm{NN}} - \frac{\varepsilon_j}{2\beta_j}| \geqslant \sqrt{\frac{P}{\gamma_{z\min}\beta_0}}$ or $\|\tilde{\omega}_j - \frac{\omega_j^*}{2}\| \geqslant \sqrt{\frac{P}{\delta_0}}$, then $\dot{V} \leqslant 0$. Then, we know that ν_j, $z_{i\mathrm{NN}}$, and $\|\tilde{\omega}_j\|$ are invariant to the sets defined as below:

$$\begin{cases}\Omega_{\nu_j} = \left(\nu_j\middle||\nu_j| \leqslant \sqrt{\dfrac{P}{k_0}} + \dfrac{\varepsilon_M}{2k_0}\right), \\ \Omega_{z_{i\mathrm{NN}}} = \left(z_{i\mathrm{NN}}\middle||z_{i\mathrm{NN}}| \leqslant \sqrt{\dfrac{P}{\gamma_{z\min}\beta_0}} + \dfrac{\varepsilon_M}{2\beta_0}\right), \\ \Omega_{\tilde{\omega}_j} = \left(\tilde{\omega}_j\middle|\|\tilde{\omega}_j\| \leqslant \sqrt{\dfrac{P}{\delta_0}} + \dfrac{\omega_{\max}}{2}\right),\end{cases} \tag{42}$$

and

$$\Omega_{\nu_2} = \left(\nu_2\middle||\nu_2| \leqslant \sqrt{\frac{P}{k_2}}\right). \tag{43}$$

So, all the signals are uniformly ultimately bounded. This completes the proof.

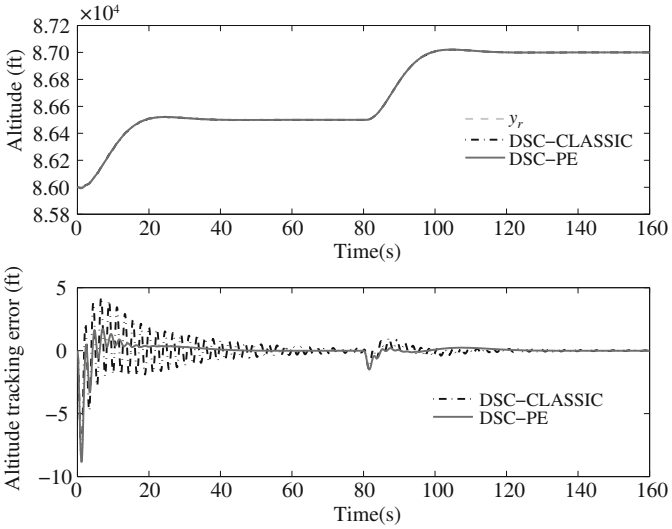

Figure 1 Altitude tracking.

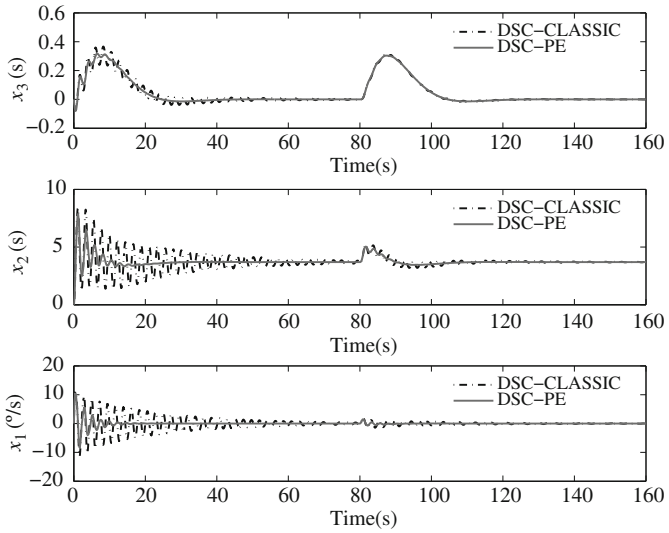

Figure 2 System states.

5 Simulation

The effectiveness and performance of the proposed controller will be verified with the simulation. For the velocity subsystem, the PID controller is employed and the parameters are selected as Kpv = 0.5, Kiv = 0.001, and Kdv = 0.01.

The initial values of the states are set as $v_0 = 7850$ ft/s, $h_0 = 86,000$ ft, $\alpha_0 = 3.5°$, $\gamma_0 = 0$, and $q_0 = 0$. The step command is $V_c = 500$ ft/s, $h_c = 1000$ ft. The reference commands of h_r and V_r are generated by the filters $\omega_{n1}\omega_{n2}^2/[(s+\omega_{n1})(s^2+2\varepsilon_c\omega_{n2}s+\omega_{n2}^2)]$ and $\omega_{v1}\omega_{v2}^2/[(s+\omega_{v1})(s^2+2\varepsilon_c\omega_{v2}s+\omega_{v2}^2)]$, respectively, where $\omega_{n1} = 0.5$, $\omega_{n2} = 0.2$, $\varepsilon_c = 0.7$, $\omega_{v1} = 0.5$, and $\omega_{v2} = 0.2$.

The control gains for the dynamic surface controller are selected as $k_h = 0.5$, $k_i = 0.05$, $k_1 = 1$, $k_2 = 2$, $k_3 = 2$. The parameters for adaptive laws are selected as $\gamma_j = 0.05I$, $\gamma_{zj} = 0.01I$, $\beta_j = 2$, $\delta_j = 0.001$, $j = 1, 3$. The filter parameters are selected as $\varepsilon_i = 0.05$, $i = 2, 3$. The number of NN nodes are set as $N_1 = 10$, $N_3 = 3^3$, with their centers x_1 and X being evenly spaced in $[-0.1; 0.1]$, $[-0.1; 0.1] \times [-0.3; 0.3] \times [-0.1; 0.1]$. To clearly show the improved tracking performance, the design in this paper is denoted as DSC-PE while the design without composite design is marked as DSC-CLASSIC. It is noted that the control parameters in DSC-CLASSIC are selected as the same as DSC-PE.

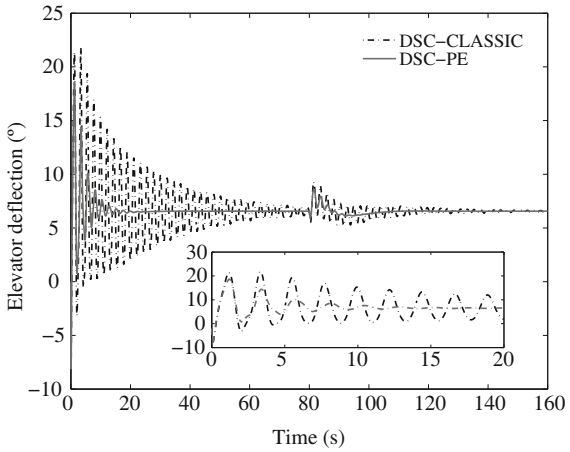

Figure 3 Elevator deflection.

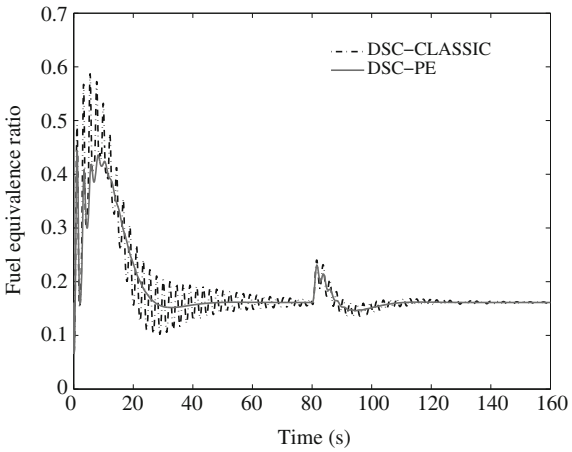

Figure 4 Fuel equivalence ratio.

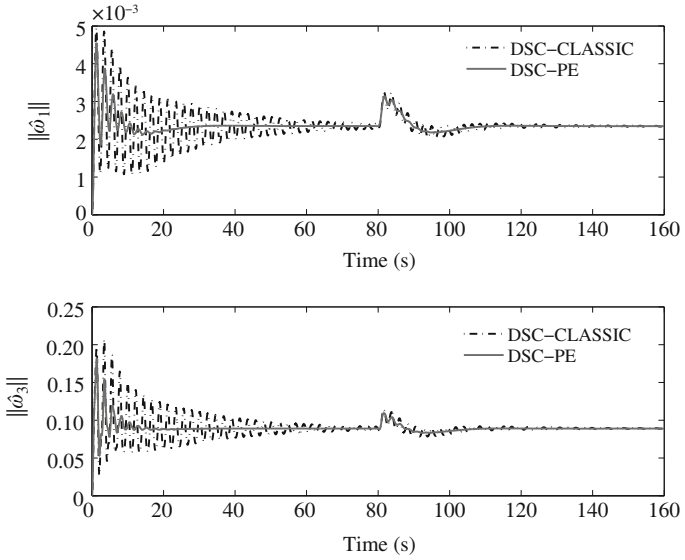

Figure 5 NN response.

The simulation results are presented in Figures 1–5. From the tracking performance shown in Figure 1, it is clearly known that the DSC design could achieve the tracking task and DSC-PE obtains better performance with less chattering. Similarly design could be found for system states in Figure 2. However, with composite design the system converges faster to the desired reference. The reason can be explained from the response of elevator deflection in Figure 3 and fuel equivalence ratio in Figure 4. From the NN response in Figure 5, it is obvious that with the information of prediction error, the neural weights exhibit smoother adaptation.

6 Conclusion

The composite neural tracking control for the longitudinal dynamics of hypersonic flight dynamics is studied in this paper. The highlight is that the composite design [24] could achieve faster NN adaptation and better tracking performance. The design is constructed with DSC scheme and composite learning, while the uniformly ultimate boundedness stability of closed-loop system is guaranteed. Simulation results of COM are presented to show the effectiveness. For future work, the flexible dynamics should be analyzed and the large envelope flight is interesting.

References

1 Xu B, Shi Z K. An overview on flight dynamics and control approaches for hypersonic vehicles. Sci China Inf Sci, 2015, 58: 070201
2 Wang Q, Stengel R. Robust nonlinear control of a hypersonic aircraft. J Guid Control Dynam, 2000, 23: 577–585
3 Dydek Z, Annaswamy A, Lavretsky E. Adaptive control and the NASA X-15-3 flight revisited. IEEE Control Syst Mag, 2010, 30: 32–48
4 Zong Q, Ji Y, Zeng F, et al. Output feedback backstepping control for a generic hypersonic vehicle via small-gain theorem. Aerosp Sci Technol, 2012, 23: 409–417
5 Chavez F R, Schmidt D K. Analytical aeropropulsive-aeroelastic hypersonic-vehicle model with dynamic analysis. J Guid Control Dynam, 1994, 17: 1308–1319
6 Parker J, Serranit A, Yurkovich S, et al. Control-oriented modeling of an airbreathing hypersonic vehicle. J Guid Control Dynam, 2007, 23: 856–869
7 Schmidt D K. Optimum mission performance and multivariable flight guidance for airbreathing launch vehicles. J Guid Control Dynam, 1997, 20: 1157–1164
8 Gibson T, Crespo L, Annaswamy A. Adaptive control of hypersonic vehicles in the presence of modeling uncertainties. In: Proceedings of American Control Conference, Saint Louis, 2009. 3178–3183
9 Xu H, Mirmirani M, Ioannou P. Adaptive sliding mode control design for a hypersonic flight vehicle. J Guid Control Dynam, 2004, 27: 829–838
10 Yang J, Li S, Sun C, et al. Nonlinear-disturbance-observer-based robust flight control for airbreathing hypersonic vehicles. IEEE Trans Aerosp Electron Syst, 2013, 49: 1263–1275
11 Yang J, Zhao Z, Li S, et al. Composite predictive flight control for airbreathing hypersonic vehicles. Int J Contr, 2014, 87: 1970–1984
12 Xu B, Gao D, Wang S. Adaptive neural control based on HGO for hypersonic flight vehicles. Sci China Inf Sci, 2011, 54: 511–520
13 Gao D, Sun Z. Fuzzy tracking control design for hypersonic vehicles via T-S model. Sci China Inf Sci, 2011, 54: 521–528
14 Farrell J, Sharma M, Polycarpou M. Backstepping-based flight control with adaptive function approximation. J Guid Control Dynam, 2005, 28: 1089–1102
15 Lee T, Kim Y. Nonlinear adaptive flight control using backstepping and neural networks controller. J Guid Control Dynam, 2001, 24: 675–682
16 Fiorentini L, Serrani A, Bolender M, et al. Nonlinear robust adaptive control of flexible air-breathing hypersonic vehicles. J Guid Control Dynam, 2009, 32: 401–416
17 Xu B, Huang X, Wang D, et al. Dynamic surface control of constrained hypersonic flight models with parameter estimation and actuator compensation. Asian J Control, 2014, 16: 162–174
18 Chen M, Ge S, How B. Robust adaptive neural network control for a class of uncertain MIMO nonlinear systems with input nonlinearities. IEEE Trans Neural Netw, 2010, 21: 796–812
19 Xu B, Sun F, Yang C, et al. Adaptive discrete-time controller design with neural network for hypersonic flight vehicle via back-stepping. Int J Contr, 2011, 84: 1543–1552
20 Xu B. Robust adaptive neural control of flexible hypersonic flight vehicle with dead-zone input nonlinearity. Nonlinear Dyn, 2014, 80: 1509–1520
21 Ge S, Hang C, Lee T. Stable Adaptive Neural Network Control. Leipzig: Springer Publishing Company, 2002. 30–31
22 Xu B, Yang C, Shi Z. Reinforcement learning output feedback NN control using deterministic learning technique. IEEE Trans Neural Netw Lear Syst, 2014, 25: 635–641
23 Gao D, Sun Z, Du T. Dynamic surface control for hypersonic aircraft using fuzzy logic system. In: Proceedings of IEEE International Conference on Automation and Logistics, Jinan, 2007. 2314–2319
24 Xu B, Shi Z, Yang C, et al. Composite neural dynamic surface control of a class of uncertain nonlinear systems in strict-feedback form. IEEE Trans Cybern, 2014, 44: 2626–2634
25 Wang L. Design and analysis of fuzzy identifiers of nonlinear dynamic systems. IEEE Trans Automat Contr, 1995, 40: 11–23
26 Narendra K, Parthasarathy K. Identification and control of dynamical systems using neural networks. IEEE Trans Neural Netw, 1990, 1: 4–27